Fabrication of stable anisotropic microcapsules

Huda A. Jerri, Rachel A. Dutter and Darrell Velegol*

Received 15th September 2008, Accepted 31st October 2008
First published as an Advance Article on the web 8th January 2009
DOI: 10.1039/b816062g

The layer-by-layer polyelectrolyte adsorption technique has been combined with the particle lithography technique to produce anisotropic polymer microcapsules each with a single nanoscale patch. The patch region covers roughly 5% of the capsule surface area, while the remaining 95% of the capsule surface is reinforced with a fluorescent nanoparticle shell. The nanoparticle shell maintains the capsule integrity and stability in suspension, while also providing a foundation for further ionic or covalent modification. The microcapsules are pH sensitive to loading and release, which we show by loading Rd6G red fluorescent dye, and they shrink and swell in response to solution pH. Confocal laser scanning microscopy confirms that these dual-functionalized capsules have a single precisely-placed nanoscale red region (revealing the underlying fluorescence) on an otherwise green surface (due to the nanoparticle coating). Even after the capsules are dehydrated, they re-hydrate intact and assume their original spherical morphology, demonstrating a resilient "Lazarus behavior". The fabrication technique avoids organic solvents, is adaptable, and produces anisotropic microcapsules that are robust to many solution conditions.

Introduction

The functionalization of microcapsules with ordered patterns or patches creates particles well suited for the fabrication of selective or targeted devices. Microcapsules that are patterned or anisotropic, however, have very seldom appeared in the literature.[1,2] One key challenge in the design of anisotropic microcapsules is the stability/robustness of the final capsules; since the capsules are hollow, they often collapse or aggregate together. Another important challenge is developing a process with the potential for scalable production. The purpose of this paper is to describe the fabrication of dual-functionalized, anisotropic microcapsules that are stable and robust in solution, even to the point of rehydrating after being completely dehydrated. The discrete patch typically covers about 5% of the capsule surface area.

Several techniques have been described previously in the literature to create anisotropic *solid* colloids, including microcontact printing with PDMS stamps loaded with surfactants or polymer particles,[3] exploitation of colloidal crystals and particle arrangements as masking substrates for patterning procedures,[4] and particle synthesis using emulsion polymerization techniques[5] and shear aggregation.[6] Charged paraffin particles have been deposited on multilayers to impact permeability, but planar substrates, not particles, were used in the literature previously.[7]

Anisotropic *capsules*, found in the literature only once due to challenges in fabrication and resuspension, have been created as Janus capsules.[2] Synthesized using layer-by-layer assembly with PDMS stamping, the capsules had different functionalizations on each hemisphere but lacked even short-term colloidal stability in DI water due to their asymmetric configurations and resulting electrostatic interactions between the oppositely-charged, large surface areas in solution. Obstacles synthesizing dual functionalities on capsules include preventing collapse, but more importantly, preventing the resulting aggregation when attractive forces are acting on considerable surface areas, in the case of opposing hemispheres. Dual functionalizations of capsules must be engineered such that the functionalizations are on distinct areas, and do not interact with each other in solution.

Our own previous work using the particle lithography technique for forming patches dealt exclusively with *solid* particles.[4,8,9] For the fabrication of patterned *capsules*, there exist several new challenges. Prominent among these are keeping the capsules stable from aggregation after fusing and obtaining low yields after settling, sonication, and centrifugation. Thus, our primary objectives were 1) to develop a simple, reproducible method for fabricating anisotropic (dual functionality), stable *microcapsules*, and 2) to demonstrate a pH-responsive loading of Rd6G dye in the resulting anisotropic microcapsules.

Unlike top-down assembly methods, the techniques used here to synthesize and modify the model particles have a path to scalable production, and yet can produce release regions down to hundreds of nanometers, generating particles potentially quite useful for applications in cosmetics, inks, sensors, or targeted delivery. The fabrication technique circumvents the use of organic solvents, and is in general safe and quite adaptable.

Materials and methods

We have fabricated our anisotropic microcapsules by combining the particle lithography technique with layer-by-layer (LbL) polyelectrolyte assembly[10] (Fig. 1). We first formed permeable, loadable polyelectrolyte capsules on sacrificial melamine formaldehyde (MF) templates, then selectively positioned nanoparticle shells over roughly 95% of each capsule. The key concept that enabled success of our process was to use a sacrificial template (*i.e.*, melamine formaldehyde), perform the processing with the template *intact*, and to remove the template only at the

Department of Chemical Engineering, The Pennsylvania State University, University Park, PA, 16802, USA. E-mail: velegol@psu.edu; Fax: +1 814-865-8739; Tel: +1 814-865-8739

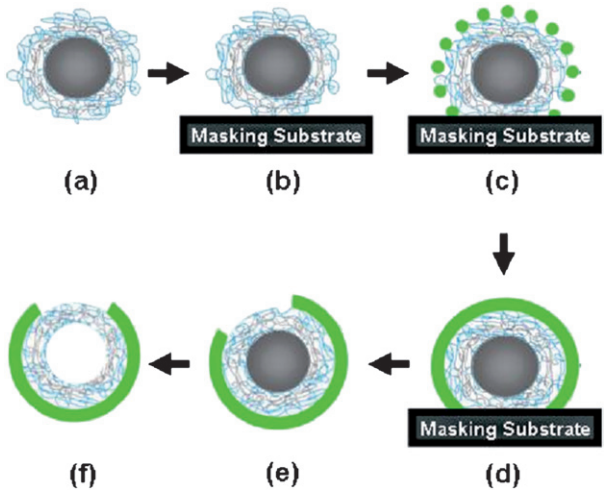

Fig. 1 Particle lithography process to create stable, dual-functionalized microcapsules. (a) A sacrificial melamine formaldehyde core particle is alternately coated with polyelectrolyte layers in solution, (b) and then settled onto an oppositely-charged masking substrate. (c) The settled particle is selectively coated with nanoparticles, which adhere to the exposed surface due to electrostatic interactions before excess particles are removed *via* rinsing. (d) A fusing step bonds the nanoparticles to the underlying polyelectrolyte multilayered particle, forming a barrier shell. (e) The selectively coated particle construction is sonicated off the substrate mask to reveal the lithographed region, (f) and is then exposed to HCl at pH 1.3 for 20 minutes to decompose the template core resulting in a hollow lithographed capsule. At this point, the hollow lithographed capsule may be loaded by incubating with dye or other ionic species.

end of the process. The different functionalities enabled imaging and provided platforms for potential further modification with electrostatic or covalent chemistry coatings.[11]

Materials

Cationic polyelectrolyte poly(allylamine hydrochloride) (PAH, M_w 70,000) and anionic poly(sodium 4-styrene sulfonate) (NaPSS, M_w 70,000) were purchased along with potassium chloride (KCl, M_w 74.5), sulfuric acid (H_2SO_4, MW 98.1), hydrochloric acid (HCl, M_w 36.46) and rhodamine 6G (Rd6G, MW 479) from Sigma-Aldrich Chemicals, USA and used without further purification. Monodisperse partially crosslinked 4.34 μm melamine formaldehyde particles (10% solids) were purchased as specialty materials from Microparticles GmbH, Berlin, Germany. Monodisperse, surfactant-free sulfate-functionalized 60 nm and 190 nm fluorescent yellow-green polystyrene latex nanoparticles (Batch No. 1-FLY-60.1 and 1-FLY-200.1 respectively) were purchased from Interfacial Dynamics Corporation (Portland, OR). A 30% solution of hydrogen peroxide (H_2O_2, MW 34.01) used for piranha etching glass substrates was purchased from VWR International. Millipore Corporation Milli-Q deionized (DI) water (resistivity roughly 18 MΩ cm) was used in all experiments.

Synthesis and loading of lithographed microcapsules

Donath and colleagues used weakly crosslinked acid-soluble melamine formaldehyde (MF) particles as sacrificial cores to form polyelectrolyte multilayered (PEM) shells with well defined wall thicknesses and core diameters.[12–15] In our work, multilayered polyelectrolyte capsules were built around sacrificial core particles and selectively coated with a barrier shell prior to a fusing step that reinforced the structure and a subsequent hollowing and incubation step that loaded the capsules with Rd6G cationic fluorescent dye (Fig. 1).

The layer-by-layer deposition of cationic and anionic polyelectrolytes in an alternating fashion was carried out using PAH and PSS as the polyelectrolyte pair. The foundations for assembly of the polyelectrolyte multilayered capsules were acid soluble partially crosslinked melamine formaldehyde (MF) cores, which decompose when subjected to pH below 1.5. This was advantageous as it bypassed the use of hydrofluoric acid or organic solvents required to decompose other core particles such as silica or polystyrene. In a 15 mL centrifuge tube, 200 μL of the 4.34 μm cationic MF particles were added to a solution containing 20 μM PSS and 30 mM KCl. The solution was left for 20 minutes to allow the PE layer to adsorb to the MF substrates. The coated particles were then centrifuged such that a pellet of particles was formed at the bottom of the tube. The supernatant was removed; the particles were resuspended in 30 mM KCl and the tube again centrifuged. This rinsing step was repeated three times to adequately remove excess PE from solution. For the third resuspension step, a solution of 20 μM PAH and 30 mM KCl was added, and the sample left for another 20 min time period so that the PAH adsorbed to the underlying polyelectrolyte coating. PSS and PAH pairs were adsorbed thus onto the MF template until a minimum of 5 PE pairs enveloped the particle. More polyelectrolyte layers could be added to tailor diffusion properties.

The addition of each polyelectrolyte layer was confirmed by zeta potential measurements. Previous observations have demonstrated that the added polyelectrolyte does not simply neutralize the surface charge, but rather imparts a positive or negative surface potential *via* charge overcompensation and charge reversal.[16–19] The terminating layer for the capsule was chosen to be PAH to facilitate adhesion for the particle lithography steps.

Once the polyelectrolyte shells were formed, the positively-charged encapsulated MF particles were settled onto negatively-charged, piranha-etched glass plates in DI water. The particles were allowed to settle for 12 hours, and then the glass dishes were gently flushed with DI water to remove any unadhered particles from the glass substrates. The DI water was replaced with 30 mM KCl solution, and fluorescent yellow-green polystyrene nanoparticles with sulfate functionality (negative charge) were introduced in excess to electrostatically adhere to the exposed particle surfaces unmasked by the glass substrate. The nanoparticles (either 60 nm or 190 nm diameter) were left to coat the particles for 12 hours, and then the plates were again rinsed with copious amounts of DI water. The lithographed particles were then fused above the glass transition temperature of the nanoparticles ($T_g \sim$ 93 °C) for 10 minutes in an autoclave (118 °C) to help anchor the nanoparticles to the polyelectrolyte capsules before rinsing and sonicating the lithographed capsules off of the glass substrate. The plates were cooled, rinsed, and sonicated for one minute to remove the lithographed particle constructions from the glass surface.

The particle suspensions were pipetted off the glass surface, and decanted into centrifuge tubes where HCl was added to decompose the core. The core dissolving procedure has been well documented, with modified methods to ensure more complete removal of the MF core.[20] The advantage of PEM shells is that they have pH dependent loading and unloading properties and the potential to induce release of core constituents under controlled or physiological conditions.[21] Loading and unloading of core constituents has been proven using spectroscopy for cores containing dyes, fluorescent probes, and small drug molecules.[22–26] We adjusted the pH to 1.3 to decompose the MF cores with a 20 minute exposure time, resulting in hollow capsules as confirmed with optical and confocal imaging. The lithographed hollow capsules were then incubated in a solution of 2.5 mM Rd6G and 30 mM KCl for 24 hours to load the capsules with fluorescent dye. The loaded capsules were rinsed with DI in three centrifugation steps to remove excess fluorescent dye and raise the pH to effectively reduce the permeability of the capsules prior to imaging.

Particle lithography was successfully used on polyelectrolyte multilayered sacrificial templates prior to fusing and sonicating steps in order to form hollow lithographed capsules. We learned that the *order* of the surface modification steps was critical, as previous attempts to lithograph pre-hollowed and loaded capsules generated low yields of fully loaded capsules. This is partly because following the settling step, the loaded capsules had a reduced surface coverage onto the glass masking substrate, resulting in significant loss of capsules after rinsing. Furthermore, the fusing step often resulted in premature unloading of the fluorescent core, whereas milder heat treatments, even with lower T_g polymers, resulted in poor adhesion of the nanoparticle coating after sonication.

From these preliminary studies we transitioned to a different strategy having determined that autoclaved, weakly crosslinked MF particles remained acid soluble following the high pressure heat treatment. With the MF core *intact*, the PE multilayered sacrificial particles were settled, lithographed, fused and then sonicated off the masking substrate. It was found that a 10 minute fusing treatment was sufficient for adherence of the nanoparticles to the polyelectrolyte multilayered core as confirmed by imaging and zeta potential measurements after sonication. Fig. 2 demonstrates that the nanoparticles are tightly bound to the polyelectrolyte capsule.

Although the time required to hollow the capsules completely increased, the acid incubation step was not long enough to weaken or collapse the capsules.

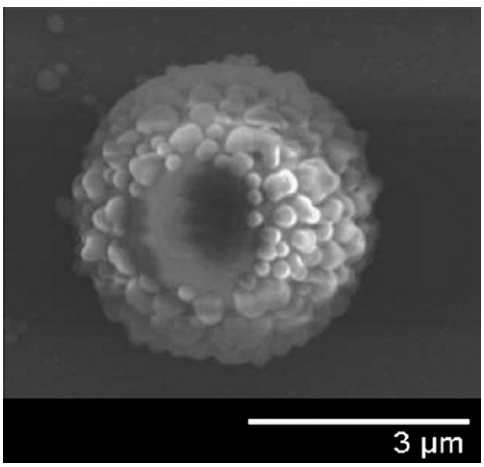

Fig. 2 Scanning electron microscope image of a 4.2 μm melamine core coated with 8 polyelectrolyte pairs and lithographed with 190 nm polystyrene nanoparticles, resulting in a 1.8 μm diameter patch, which closely matches predicted patch size of 1.79 μm. This image shows that the nanoparticles are tightly bound to the underlying substrate, and the patch region is preserved after sonication and drying. The construction was imaged with the core intact using a scanning electron microscope and an accelerating voltage of 5 kV.

Dehydration and rehydration of "Lazarus microcapsules"

The collapsed structure of microcapsules after dehydration has been clearly presented in the literature, where scanning electron microscopy shows the defined folds and film architecture of dried capsules.[27–29] For our work, rehydration studies were performed to examine the differences in behavior between hollow *lithographed* microcapsules and *unlithographed* control microcapsules exposed to identical fusing, hollowing and sonication conditions. LbL polyelectrolyte deposition was performed as detailed above for the control particles, with a 24 hour incubation step in Rd6G to tag the ninth anionic layer. Twelve layers were added and the cationic particles were settled onto piranha-etched glass plates. 30 mM KCl was then added to the glass plates, and 60 nm FYG nanoparticles were used to lithograph half of the samples. Both the lithographed and control particle batches were then carefully rinsed, fused, sonicated and hollowed prior to the studies. Droplets of the hollow lithographed and control particle solutions were pipetted onto respective glass coverslips and allowed to air dry for 24 hours. Both capsule constructions were examined in their collapsed state and following the addition of DI water using an inverted optical microscope.

Equipment and characterization

Confocal and DIC optical microscopy images were captured on an Olympus Fluoview 1000 Confocal Laser Scanning Microscope with a 60× oil objective at the Huck Institute of the Life Sciences Center for Quantitative Cell Analysis. Rehydration study images were taken using a Nikon Eclipse TE2000-U Inverted Optical Microscope with a 100× oil objective. Fusing steps were performed using a standard steam autoclave at 120 °C. A standard swing bucket centrifuge was used for particle separation and rinsing. The ultrasonicator was purchased from VWR International (Model 550T), and zeta potential measurements were taken using a Zeta Potential Utilizing Phase Analysis Light Scattering instrument (ZetaPALS) from Brookhaven Instruments Corporation. FTIR spectra were gathered using a Thermo Nicolet Nexus 670 FT-IR instrument, and samples were dried onto KBr pellets and analyzed using 75 scans and a DTGS KBr detector.

Results and discussion

Fabrication of stable, loaded dual functionalized capsules

The capsule hollowing step was imaged for an acid soluble MF core with 8 polyelectrolyte layers lithographed with 190 nm

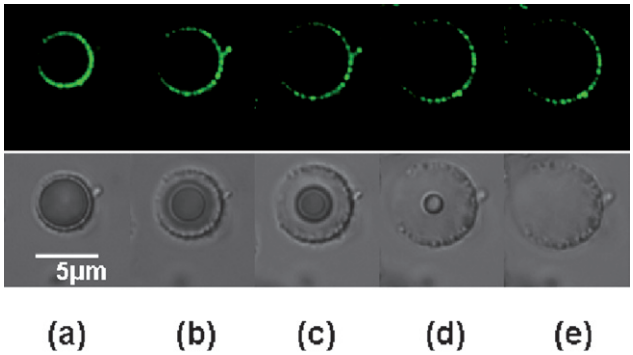

Fig. 3 Confocal microscope time lapse images of dissolution of sacrificial template core to form lithographed capsules. The sequence was imaged upon addition of HCl to adjust the solution pH of MF(PSS/PAH)$_4$ lithographed with 190 nm FYG (after 10 min of autoclave fusing) to pH 1.3 after (a) 0 min, (b) 2 min, (c) 10 min, (d) 15 min and (e) 20 min respectively. The lithographed shell and single patch region remain intact during hollowing as capsule swells in response to pH drop.

fluorescent yellow green nanoparticles (Fig. 3). It was observed that the MF core particle dissolved centro-symmetrically when the solution pH was adjusted to 1.3, and that the capsule swelled in response to the pH drop as expected, likely due to the osmotic forces[20] resulting from the melamine formaldehyde oligomers formed during decomposition.

The nanoparticle shell, which covered roughly 95% of the surface area of each particle, was robust enough to swell with the underlying capsule substrate in response to the pH drop. This is seen in the confocal image sequence of the core dissolution (upper half of Fig. 3b–e). The polyelectrolyte shell swells approximately 35% from the original inner diameter measurement (Fig. 3a) to the completely swollen capsule incubated at pH 1.3 for 20 minutes (Fig. 3e). For bulk samples where several rinsing steps were used to remove the melamine formaldehyde degradation products and raise the pH, it was found that the resuspended lithographed capsules responded to the pH increase by decreasing in size and returned to the same size and morphology as unlithographed control samples under identical solution conditions. This is illustrated in Fig. 4, where hollowed and rinsed capsules made of 5 bilayers and lithographed with 60 nm fluorescent yellow green nanoparticles were resuspended in solutions with pH adjusted between 2 and 6 prior to imaging. As the pH was raised, the approximate inner diameter of the capsules was reduced from 6.0 μm in pH 1.3 solution to 4.4 μm in pH 2.5 and roughly 4.0 μm in pH 3.5 and 5.5 respectively.

FTIR analysis was performed to determine the extent of core product removal. The spectra in Fig. 5 were compared to spectra for standard MF cores, PAH and PSS used to fabricate capsules and capsules before and after the acid dissolution step. The characteristic peaks from the PAH and PSS shell materials (amine peaks due to stretching and bending vibrations at 3237–3556 cm^{-1} and 1517 cm^{-1} respectively) are consistent before and after acid dissolution, whereas the spectral range of 1400 to 800 cm^{-1}, which includes the C–N–C peak at 807 cm^{-1} and the C–O–C peaks in the range of 1022 to 1095 cm^{-1} associated with the core material, show essentially 100% transmittance after core removal, indicating that the core is mostly removed.

Once it was confirmed that the core material was adequately removed, the hollow capsules were incubated with Rd6G fluorescent red dye for 24 hours, followed by three rinsing steps. The result was the synthesis of stable, free-floating, loaded lithographed capsules, where the selectively-placed barrier shell around the permeable polyelectrolyte multilayered capsule offers

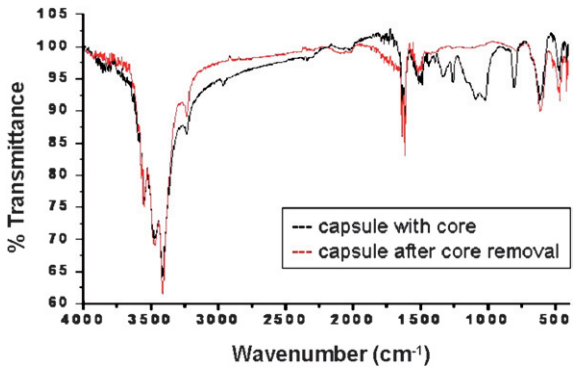

Fig. 5 FTIR spectra for capsules before and after the acid dissolution step to evacuate the capsule cores show that core is mostly removed. 75 scans were collected to give an average spectrum with a resolution of 4. The black plot corresponds to the capsules with the core material intact, and the red plot shows the absence of the cores' characteristic peaks following core removal.

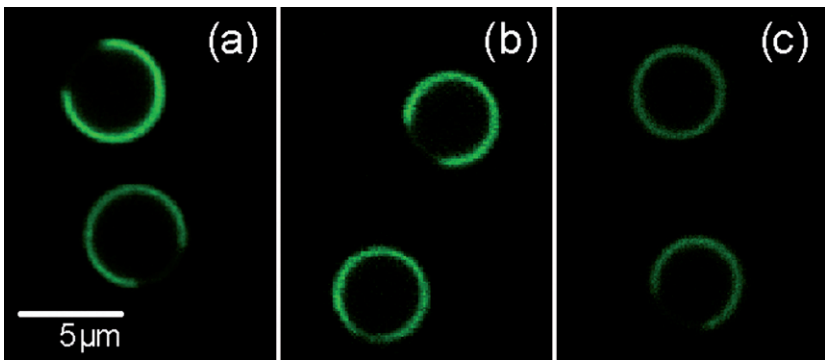

Fig. 4 CLSM images of (PSS/PAH)$_5$ hollow capsules shrinking in response to increasing pH. Capsules were lithographed with 60 nm fluorescent yellow green nanoparticles and resuspended in acidic HCl solutions adjusted to (a) pH 2.5, (b) 3.5 and (c) 5.5 respectively with HCl. The barrier shells remained intact as the inner diameter decreased approximately 9%.

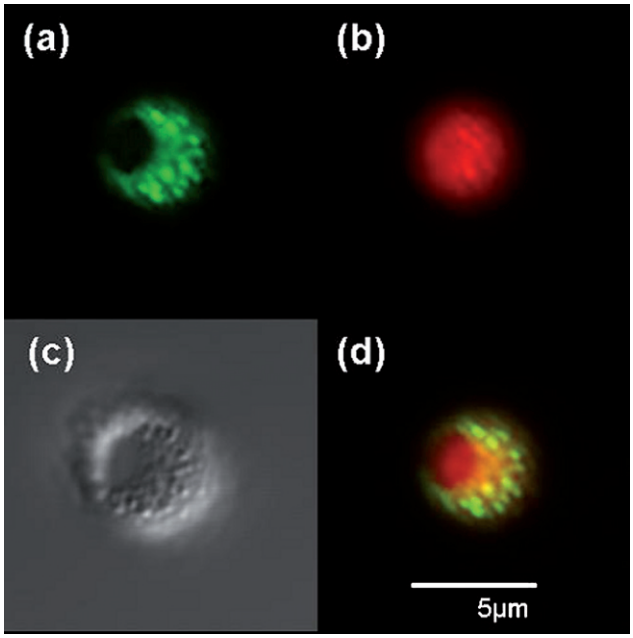

Fig. 6 Hollow lithographed capsules uptake and retain dyes after fusing step as demonstrated in this CLSM image. The image is a 60× oil magnification of a $(PSS/PAH)_5$ capsule lithographed with a 190 nm fluorescent yellow green nanoparticle shell and loaded with fluorescent red Rd6G cationic dye molecules. Sequential scanning shows the individual components of the lithographed capsule. (a) The blue laser excitation shows the green lithographed shell, with the lithographed "hole" in the green shell of nanoparticles. (b) The green laser excitation shows the red dye loaded into the hollow capsule. Both the (c) DIC image and (d) confocal overlay of the lithographed shell onto the loaded capsule reveal the dual functionalizations of the anisotropic capsule.

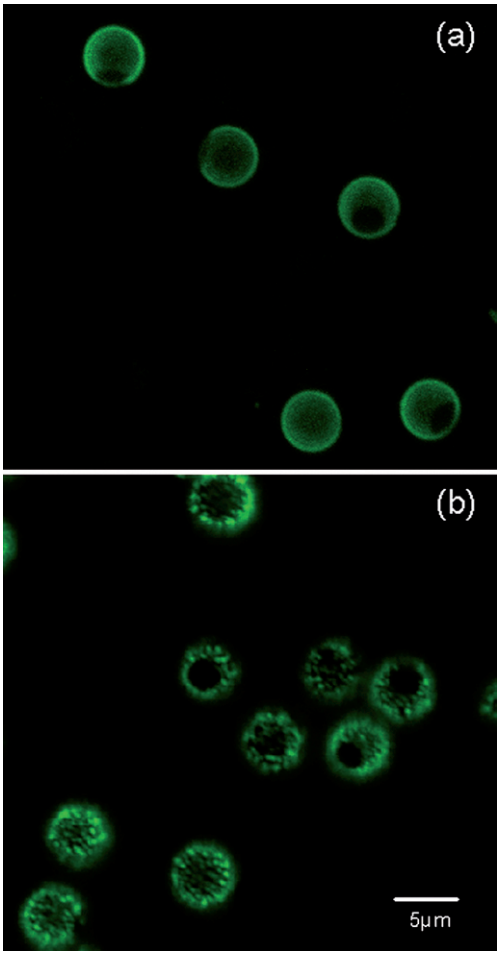

Fig. 7 Coating particle sizes influence coarseness of shell and patch region as shown in these CLSM images at 60× oil magnification of $(PSS/PAH)_5$ hollow capsules lithographed with (a) 60 nm and (b) 190 nm fluorescent yellow green particles.

supplemental imaging capabilities and serves as an orientation device by clearly showing the location of the lithographed region (Fig. 6). No visible aggregation or collapse, assessed using an optical microscope, was observed for various lithographed capsule samples stored in deionized water up to 14 months. Successful loading of the capsules showed that the fusing step did not damage capsule integrity or irreversibly reduce permeability, which might otherwise have prevented uptake of ionic dyes or other molecules.

Fig. 6 and similar images confirm placement of the localized bare patch, the size of which corresponds closely to the size predicted from simple geometric considerations based on the core and coating particle sizes.[8] The size of the lithographed region can be fine tuned as shown in Fig. 7, where capsules were lithographed with 60 nm or 190 nm fluorescent yellow green nanoparticles respectively and resuspended under similar conditions prior to imaging.

The capsule lithography procedure offers versatility in terms of fabrication as the patch region size is controlled by varying the size of the coating nanoparticles. For the samples imaged in Fig. 7, the capsules lithographed with 60 nm particles have an estimated average diameter of 4.8 μm and a 2.0 μm ± 186 nm patch size, whereas the capsules lithographed with 190 nm particles have an estimated average diameter of 5.4 μm and patch size of 2.4 μm ± 93 nm, with an imaging resolution of approximately 200 nm for confocal microscopy. The patch sizes for lithographed capsules are larger than the predicted values for rigid spheres. This is somewhat surprising, since predictions for the patch size on rigid spheres have always matched our experimental observations. We do not fully understand the difference for capsules, although we can speculate that it is due to their deformability. The size of the nanoparticles chosen for lithographing the capsules can be used to significantly augment or fine tune wall thickness and patch size, and the choice also has a bearing on the overall surface charge of the particle constructions as confirmed by zeta potential measurements. Capsules of $MF(PSS/PAH)_9$ with the template intact and lithographed with either 60 nm or 190 nm sulfate functionalized nanoparticles gave zeta potential readings of -25 ± 1.2 mV and -34 ± 0.5 mV while suspended in pH 5 adjusted DI. These measurements were found using a ZetaPALS instrument by taking 5 runs with 15 measurement cycles per run, using the Smoluchowski model for electrophoresis. In contrast, bare acid-soluble MF templates were measured to have a zeta potential value of 92 ± 1.4 mV. The thickness of the lithographed shell influenced the surface charge as expected and indicated that the lithographed shells survive sonication, protect the underlying capsules, electrostatically stabilize the constructions and are sufficiently charged to serve as reliable foundations for surface modulation.

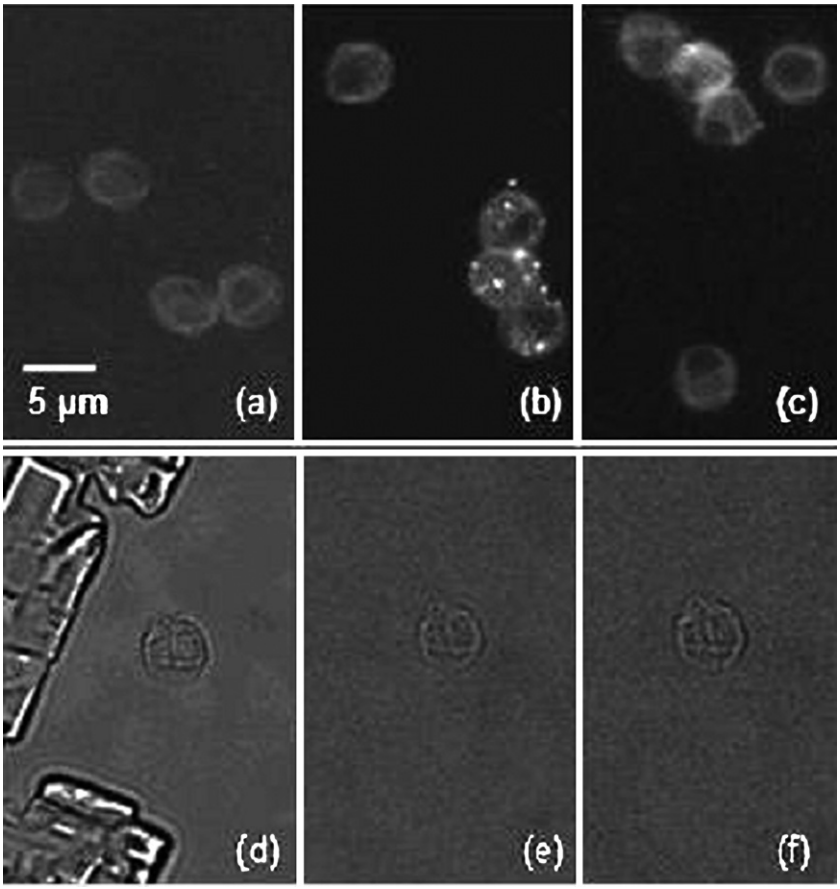

Fig. 8 Time lapse rehydration sequences for rehydratable microcapsules (top) and bare control capsules (bottom) in their collapsed and rehydrated configurations imaged using an inverted optical microscope. Hollow lithographed microcapsule $(PSS/PAH)_6$ solution was pipetted onto coverslips and imaged (a) dried and completely collapsed, (b) blooming after rehydration for 20 min with DI water (c) mostly spherical with lithographed patch intact after rehydration for 35 min with DI water. The second row of bare control microcapsules illustrates (d) dried and collapsed on the substrate, (e) after rehydration for 25 minutes with DI water and (f) following 120 min rehydration session. The control capsules show no noticeable rehydration. Bare capsules remained collapsed during the entire 3 hour imaging session.

With the permanently-bound shell protecting the sensitive underlying capsules in solution, the final study was to investigate the effects of dehydration on the capsules. The ability to dry and later restore capsules could be important for applications requiring storage, especially if the capsule or its contents are subject to degradation if they are stored in aqueous media. The lithographed shell was observed not only to stabilize the colloidal dispersion from aggregating in suspension (due to having adequate repulsive interactions), but the shell also gave the capsules sufficient mechanical integrity to rehydrate after being shriveled. The lithographed and control microcapsules were imaged in their desiccated and rehydrated states, as shown in Fig. 8. AFM analysis was attempted, but images were poor due to the surface roughness and height (greater than 1.5 μm) of the collapsed lithographed capsules.

Upon the addition of DI water, the collapsed lithographed capsules swelled to assume a mostly spherical shape with small folds apparent in many of the particles. Following ten minutes, the lithographed capsules detached from the glass imaging substrate, likely due to electrosteric repulsion from the anionic nanoparticle shell. The free-floating, dual-functionalized microcapsules revived to resemble their original morphology in suspension after an approximately 20 minute rehydration time, showing a type of "Lazarus functionality". In contrast, the similarly-fused and heat-treated unlithographed control capsules remained strongly anchored to the glass substrate, and did not demonstrate any noticeable swelling or unfolding several hours after the rehydration step. A final testament to the versatility of the anisotropic fabrication process stems from results showing fused lithographed and unlithographed control capsules able to withstand a minimum of 5 hours incubated in pH 12 NaOH solutions without noticeable dissociation, deformation, or aggregation. These results strongly suggest that lithographed microcapsules are robust enough to survive further modification with covalent chemistries, thus serving as environment-responsive cores for more complex functionalizations, assemblies and colloidal devices.

Conclusions

In this paper our primary purpose was to fabricate anisotropically-functionalized loadable, polyelectrolyte multilayered hollow microcapsules having dual chemistries. The size of the patch region, typically 5% of the surface area, can be well

controlled, and the capsules were robust and stable to aggregation, sonication, and even dehydration. Although the nanoparticle-coated capsules are considerably more resilient than the unlithographed control capsules, the fabrication process is gentle and provides flexibility in terms of materials, wall thicknesses and patch size while circumventing the use of organic solvents.

Our current aims focus on two points. First, we are investigating how to produce a coating on the particle that has no "pinholes" such that core constituents are forced to evacuate through the lithographed patch in a focused manner. We have employed other polymer colloids and coating layers, and now we are investigating some fundamental issues of polymer spreading at temperatures above T_g in order to identify feasible combinations of polymer colloids, solvent type and quality, and coating layers. Lithography with initiator, followed by modified emulsion polymerization techniques has led to the formation of homogenous polystyrene barrier shells. Our work is moving to known biocompatible polyelectrolytes and biodegradable nanoparticles, creating impermeable shells using chemical crosslinking strategies,[30,31] multi-particle layering, and modified emulsion polymerization and ATRP or "living" polymerization methods to significantly reduce permeability of the barrier shell. Second, scalable production is required for applications we envision in anisotropic polyelectrolyte reservoir systems,[32] which will be useful as cartridges to be loaded and unloaded with dyes or functional molecules in response to solution pH at targeted sites or organelles. Our technique has the potential for scalability, by replacing the flat substrate for particle lithography with ~10 μm particles as the "flat surfaces", thus making the full 3-dimensional volume of a container accessible for processing. The engineering science challenges for scalability include mixing, evaluating time scales, and separations.

Acknowledgements

We thank the National Science Foundation (CBET Grant #0651611) for funding this work. We also thank the Huck Institute of Life Sciences Center for Qualitative Cell Analysis for use of the Olympus Fluoview 1000 confocal laser scanning microscope (through a project funded in part under a grant with the Pennsylvania Department of Health using Tobacco Settlement Funds) and their continued support with imaging and analysis, as well as the Penn State Materials Research Laboratory particle characterization laboratory for help generating zeta potential measurements and particle size distributions. Erik Hsiao and Anna Barnette are thanked for their efforts generating and evaluating the FTIR spectra. Finally, Drs. Allison Yake and Charles Snyder are greatly appreciated for their collaborative spirit and advice regarding particle functionalization and stability.

References

1 Z. Zhang and S. C. Glotzer, Self-Assembly of Patchy Particles, *Nano Letters*, 2004, **4**(8), 1407–1413.
2 Z. Li, D. Lee, M. F. Rubner and R. E. Cohen, Layer-by-Layer Assembled Janus Microcapsules, *Macromolecules*, 2005, **38**, 7876–7879.
3 O. Cayre, V. N. Paunov and O. D. Velev, Fabrication of Asymmetrically Coated Colloid Particles by Microcontact Printing Techniques, *Journal of Materials Chemistry*, 2003, **13**, 2445–2450.
4 C. E. Snyder, A. M. Yake, J. D. Feick and D. Velegol, Nanoscale Functionalization and Site-Specific Assembly of Colloids by Particle Lithography, *Langmuir*, 2005, **21**, 4813–4815.
5 V. N. Manoharan, M. T. Elsesser and D. J. Pine, *Science*, 2003, **301**, 483–487.
6 P. M. Johnson, C. M. vanKats and A. van Blaaderen, *Langmuir*, 2005, **21**, 11510–11517.
7 K. Glinel, M. Prevot, R. Krustev, G. B. Sukhorukov, A. M. Jonas and H. Mohwald, Control of the Water Permeability of Polyelectrolyte Multilayers by Deposition of Charged Paraffin Particles, *Langmuir*, 2004, **20**, 4898–4902.
8 A. M. Yake, C. E. Snyder and D. Velegol, Site Specific Functionalization on Individual Colloids: Size Control, Stability and Multilayers, *Langmuir*, 2007, **23**, 9069–9075.
9 A. M. Yake, A. S. Zahr, H. A. Jerri, M. V. Pishko and D. Velegol, Localized functionalization of individual colloidal carriers for cell targeting and imaging, *Biomacromolecules*, 2007, **8**(6), 1958–1965.
10 G. Decher and J. D. Hong, Buildup of Ultrathin Multilayer Films by a Self-Assembly Process, *International Journal of Physical Chemistry*, 1991, **95**(11), 1430–1434.
11 A. M. Yake, C. E. Snyder and D. Velegol, Site-Specific Functionalization on Individual Colloids: Size Control, Stability and Multilayers, *Langmuir*, 2007.
12 E. Donath, G. B. Sukhorukov, F. Caruso, S. A. Davis and H. Mohwald, Novel Hollow Polymer Shells by Colloid-Templated Assembly of Polyelectrolytes, *Angewandte Chemie*, 1998, **37**(16), 2202–2205.
13 F. Caruso, Hollow Capsule Processing through Colloidal Templating and Self-Assembly, *Chem. Eur. J.*, 2000, **6**(3), 413–419.
14 F. Caruso, R. A. Caruso and H. Mohwald, Nanoengineering of Inorganic and Hybrid Hollow Spheres by Colloidal Templating, *Science*, 1998, 282.
15 G. B. Sukhorukov, E. Donath, S. Davis, H. Lichtenfeld, F. Caruso, V. I. Popov and H. Mohwald, Stepwise Polyelectrolyte Assembly on Particle Surfaces: a Novel Approach to Colloid Design, *Polymers for Advanced Technologies*, 1998, **9**, 759–767.
16 J. B. Schlenoff and S. T. Dubas, Mechanism of Polyelectrolyte Multilayer Growth: Charge Overcompensation and Distribution, *Macromolecules*, 2001, **34**, 592–598.
17 K. S. Birdi, *Handbook of Surface and Colloid Chemistry*, 2nd edn, CRC Press, Boca Raton, 2003.
18 E. Blomberg, E. Poptoshev and F. Caruso, Surface Interactions during Polyelectrolyte Multilayer Build-Up. 2. The Effect of Ionic Strength on the Structure of Preformed Multilayers, *Langmuir*, 2006, **22**, 4153–4157.
19 R. Podgornik, T. Akesson and B. Jonsson, Colloidal Interaction Mediated *via* Polyelectrolytes, *J. Chem. Phys.*, 1995, **102**(23), 9423–9434.
20 C. Gao, S. Moya, H. Lichtenfeld, A. Casoli, H. Fiedler, E. Donath and H. Mohwald, The Decomposition Process of Melamine Formaldehyde Cores: The Key Step in the Fabrication of Ultrathin Polyelectrolyte Multilayer Capsules, *Macromolecular Materials and Engineering*, 2001, **286**(6), 355–361.
21 D. M. Lynn, M. M. Mamiji and R. Langer, pH-Responsive Polymer Microspheres: Rapid Release of Encapsulated Material within the Range of Intracellular pH, *Angew. Chem. Int. Ed.*, 2001, **40**(9), 1707–1710.
22 A. A. Antipov and G. B. Sukhorukov, Polyelectrolyte Multilayer Capsules as Vehicles with Tunable Permeabilitiy, *Advances in Colloid and Interface Science*, 2004, **111**, 49–61.
23 S. E. Burke and J. Barrett, pH Dependent Loading and Release Behavior of Small Hydrophilic Molecules in Weak Polyelectrolyte Multilayer Films, *Macromolecules*, 2004, **37**, 5375–5384.
24 A. J. Chung and M. F. Rubner, Methods of Loading and Releasing Low Molecular Weight Cationic Molecules in Weak Polyelectrolyte Multilayer Films, *Langmuir*, 2002, **18**, 1176–1183.
25 E. Nicol, J. L. Habib-Jiwan and A. M. Jonas, Polyelectrolyte Multilayers as Nanocontainers for Functional Hydrophilic Molecules, *Langmuir*, 2003, **19**, 6178–6186.
26 W. Tong, W. Dong, C. Gao and H. Mohwald, Charge-Controlled Permeability of Polyelectrolyte Microcapsules, *J. Phys. Chem. B*, 2005, **109**, 13159–13165.
27 O. V. Lebedeva, B.-S. Kim, K. Vasilev and O. I. Vinogradova, Salt Softening of Polyelectrolyte Multilayer Microcapsules, *Journal of Colloid and Interface Science*, 2005, **284**, 455–462.

28 G. B. Sukhorukov, D. G. Shchukin, W.-F. Dong, H. Mohwald, Lulevich and O. I. Vinogradova, Comparative Analysis of Hollow and Filled Polyelectrolyte Microcapsules Templated on Melamine Formaldehyde and Carbonate Cores, *Macromolecular Chemistry and Physics*, 2003, **205**, 530–535.
29 C. Gao, S. Leporatti, S. Moya, E. Donath and H. Mohwald, Swelling and Shrinking of Polyelectrolyte Microcapsules in Response to Changes in Temperature and Ionic Strength, *Chem. Eur. J.*, 2003, **9**(4), 915–920.
30 L. Richert, F. Boulmedais, P. Lavalle, J. Mutterer, E. Ferreux, G. Decher, P. Schaaf, J.-C. Voegel and C. Picart, Improvement of Stability and Cell Adhesion Properties of Polyelectrolyte Multilayer Films by Chemical Cross-Linking, *Biomacromolecules*, 2004, **5**, 284–294.
31 W. Tong, C. Gao and H. Mohwald, Manipulating the Properties of Polyelectrolyte Microcapsules by Glutaraldehyde Cross-Linking, *Chem. Mater.*, 2005, **17**, 4610–4616.
32 R. Langer, Polymer-Controlled Drug Delivery, *Acc. Chem. Res.*, 1993, **26**, 537–542.

